**IOSR Journal of Engineering (IOSRJEN)** **www.iosrjen.org**
ISSN (e): 2250-3021, ISSN (p): 2278-8719
Vol. 09, Issue 12, December. 2019, ||Series -I || PP 28-37

# sd-Hybridization, Population Analysis And MOT In $Ru^{2+}$. I. Simple Ruthenium Dihalides

**Alok Shukla[1], Kavindra Kumar Mishra[2] and Anil Kumar Soni[3*]**
*[1]Department of Physics, Maharani LalKunwari, P.G. College, Balrampur (U.P.), India*
*[2]Department of Physics, Mewar University, Chittorgarh, Rajasthan, India*
*[3]Department of Chemistry, Shia P.G. College, Sitapur Road, Lucknow (U.P.), India*
*Corresponding Author: Anil Kumar Soni*
*Received 28 November 2019; Accepted 13 December 2019*

**Abstract:** Atomic orbital (AO) and molecular orbital (MO) treatment has been made on ruthenium(II) halides: $RuCl_2$, $RuBr_2$, and $RuI_2$. The $\sum c_i$values 4dx2-y2, 4dxz, 4dxy, 5s, 5px, 5py, 5pzAOs of metal in their halides show sd-hybridization, which is supported by their bond angles as proposed by Landis et al. Further, $\sum c_i$values are highest in case of iodide and lowest in chloride shows good agreement with nephelauxetic series of ligands i.e. the effective positive charge on Ru is reduced greater by iodide and lesser by chloride, while bromide lies in between them. Population analysis study shows among the seventeen ($\phi_{1}$–$\phi_{17}$) MOs formed by LCAO-MO approximation, nine ($\phi_1$–$\phi_5$ and $\phi_8$–$\phi_{11}$) are bonding, two ($\phi_6$ and $\phi_7$) are nonbonding and remaining six ($\phi_{12}$–$\phi_{17}$) are antibonding. The nonbonding MOs, $\phi_6$ and $\phi_7$, are purely 4dyx and $4dz^2$ AOs of ruthenium, respectively. The magnitude of splitting of ruthenium's d-orbitals has also been studied that follow the sequence $RuCl_2 > RuBr_2 > RuI_2$, which is in good agreement with spectrochemical series of ligands i.e. larger splitting by chloride and shorter by iodide, and bromide in between them. The MOT reflected that all the MOs ($\phi_1$–$\phi_{17}$) have definite energy and definite shape due to (a) different contribution ($c_{ri}$ and $c_{si}$) of many basis functions ($\chi_1$–$\chi_{17}$), (b) difference in energies ($\Delta\varepsilon$) of overlaping AOs, (c) difference in overlap integral ($S_{r\text{-}s}$) and (d) symmetry (phase) of overlapping AOs. And, thus provide clear cut electronic picture of the molecule, which more precisely explain or help to explain the various properties of the molecule.

**Key-words:** Simple ruthenium dihalides, Atomic orbital treatment, Molecular orbital treatment and Mulliken population analysis

## I. INTRODUCTION

A quantitative atomic orbital (AO) and molecular orbital (MO) treatment has been made on Ruthenium(II) halides to study (i) involvement of metal (n-1)d-, ns-and np-orbitals in hybridizations and its type that provide information related to shape (bond angle) and size (bond length); (ii) contribution of various AOs in the formation of MOs through LCAO approximation using values of eigenvector and overlap matrix; (iii) nature of MOs by distinguishing them in to bonding, nonbonding and antibonding MOs through population analysis; and (v) splitting of metal (n-1)d-orbitals and its magnitude.

## II. MATERIAL AND METHODS

The study materials of this research work are $RuCl_2$, $RuBr_2$ and $RuI_2$. The 3D modeling and geometry optimization of the halides have been done by CAChe software using molecular mechanics with EHT option [1]. Eigenvectors, overlap matrix and eigenvalues have been computed with the same software, using the same option. The method adopted for various calculations are based on Mulliken population analysis (MPA) [2]. Within the LCAO-MO approximation, the wave function for i<sup>th</sup> eigen state of molecule as defined by Mulliken is

$$\phi_i = \sum_{rk} c_{irk}\chi_{rk} \qquad \text{Eq. 1}$$

The contributions of electrons ($n_{r,i}$) in each occupied MO are calculated by using the following equation as proposed by Mulliken

$$n_{r,i} = n_i c_{ri}^2 \qquad \text{Eq. 2}$$

where $n_i$ is the number of electron in MO $\phi_i$ and $c_{ri}$ is the coefficient of AOs for MO $\phi_i$ ($i = 1-17$). Thereafter, MPA has also used for evaluating overlap population as described below

$$n_{r-s,i} = n_i(2c_{ri}c_{si}S_{rs}) \qquad \text{Eq. 3}$$

where, $c_{ri}$ is the coefficient of atomic orbitals for one atom, $c_{si}$ is the coefficient of AOs for other atom and $S_{rs}$ is the overlap integral between the two AOs (one of an atom and one of other atom).

## III. RESULTS AND DISCUSSION

A systematic molecular mechanics based investigation of bonding nature in ruthenium dihalides has been studied. Ruthenium dihalides, which are under investigation, are dichloride, dibromide and diiodide, except difluoride, which does not exist.

### 3.1 Ruthenium dichloride

Ruthenium(II) chloride is triatomic molecule, having the following optimized geometry as obtained from molecular mechanics method.

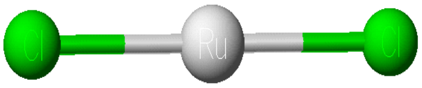

Bond Length=2.238Å

Bond Angle=179.99$^0$

**Fig. 1 Structure of RuCl$_2$**

The MOs of this molecule are formed by linear combination of 17AOs: nine orbitals (five 4d-orbitals, one 5s orbital and three 5p orbitals) from ruthenium and four orbitals (three 3p orbitals and one 3s orbital) from each chlorine atom. These are AOs are represented by $\chi$. These are $\chi_1$ = 5s, $\chi_2$ = 5px, $\chi_3$ = 5py, $\chi_4$ = 5pz, $\chi_5$ = 4dx$^2$-y$^2$, $\chi_6$ = 4dz2, $\chi_7$ = 4dxy, $\chi_8$ = 4dxz, $\chi_9$ = 4dyz, for Ru-1 and $\chi_{10}$ = 3s, $\chi_{11}$ = 3px, $\chi_{12}$ = 3py, $\chi_{13}$ = 3pz for Cl-2 and $\chi_{14}$ = 3s, $\chi_{15}$ = 3px, $\chi_{16}$ = 3py, $\chi_{17}$ = 3pz for Cl-3). These 17 AOs on LCAO approximations give 17 MOs (represented by $\phi_1$ to $\phi_{17}$). The magnitude of contribution of various AOs ($\chi$) in the formation of 17 MOs is demonstrated by Eqs., $\phi_1$ to $\phi_{17}$.Here, the coefficients of $\chi$ are the eigenvector and its zero or near zero values have been omitted.

$\phi_1 = -0.1029\chi_1 - 0.1034\chi_5 + 0.0606\chi_6 - 0.0181\chi_7 - 0.6626\chi_{10} - 0.0142\chi_{11} - 0.0012\chi_{12} - 0.6626\chi_{14} + 0.0142\chi_{15} + 0.0012\chi_{16}$

$\phi_2 = 0.0686\chi_2 + 0.0060\chi_3 + 0.6829\chi_{10} + 0.0187\chi_{11} + 0.0016\chi_{12} - 0.6829\chi_{14} + 0.0187\chi_{15} + 0.0016\chi_{16}$

$\phi_3 = -0.0966\chi_1 - 0.4559\chi_5 + 0.2672\chi_6 - 0.0799\chi_7 - 0.1572\chi_{10} + 0.4899\chi_{11} + 0.0426\chi_{12} + 0.1572\chi_{14} - 0.4899\chi_{15} - 0.0426\chi_{16}$

$\phi_4 = -0.0001\chi_5 + 0.0008\chi_7 - 0.7490\chi_8 - 0.0651\chi_9 + 0.0004\chi_{12} - 0.4021\chi_{13} - 0.0004\chi_{16} + 0.4021\chi_{17}$

$\phi_5 = -0.1298\chi_5 + 0.7405\chi_7 + 0.0008\chi_8 + 0.0001\chi_9 - 0.0348\chi_{11} + 0.4006\chi_{12} + 0.0004\chi_{13} + 0.0348\chi_{15} - 0.4006\chi_{16} - 0.0004\chi_{17}$

$\phi_6 = 0.0866\chi_8 - 0.9962\chi_9$

$\phi_7 = 0.4925\chi_5 + 0.8660\chi_6 + 0.0863\chi_7$

$\phi_8 = -0.1675\chi_2 - 0.0146\chi_3 + 0.0675\chi_{10} + 0.6380\chi_{11} + 0.0555\chi_{12} - 0.0675\chi_{14} + 0.6380\chi_{15} + 0.0555\chi_{16}$

$\phi_9 = -0.0110\chi_2 - 0.1267\chi_3 + 0.0004\chi_4 + 0.0589\chi_{11} - 0.6770\chi_{12} + 0.0023\chi_{13} + 0.0589\chi_{15} - 0.6770\chi_{16} + 0.0023\chi_{17}$

$\phi_{10} = -0.0004\chi_3 - 0.1272\chi_4 + 0.0002\chi_{11} - 0.0023\chi_{12} - 0.6796\chi_{13} + 0.0002\chi_{15} - 0.0023\chi_{16} - 0.6796\chi_{17}$

$\phi_{11} = 0.4603\chi_1 - 0.6570\chi_5 + 0.3851\chi_6 - 0.1151\chi_7 + 0.0028\chi_{10} - 0.2801\chi_{11} - 0.0244\chi_{12} + 0.0028\chi_{14} + 0.2801\chi_{15} + 0.0244\chi_{16}$

$\phi_{12} = -0.0001\chi_5 + 0.0007\chi_7 + 0.6699\chi_8 + 0.0583\chi_9 + 0.0001\chi_{11} - 0.0006\chi_{12} - 0.5895\chi_{13} - 0.0001\chi_{15} + 0.0006\chi_{16} + 0.5896\chi_{17}$

$\phi_{13} = 0.1161\chi_5 - 0.6623\chi_7 + 0.0007\chi_8 + 0.0001\chi_9 - 0.0511\chi_{11} + 0.5873\chi_{12} - 0.0006\chi_{13} + 0.0511\chi_{15} - 0.5873\chi_{16} + 0.0006\chi_{17}$

$\phi_{14} = 0.0886\chi_2 - 1.0188\chi_3 - 0.0030\chi_4 - 0.0227\chi_{11} + 0.2608\chi_{12} + 0.0008\chi_{13} - 0.0227\chi_{15} + 0.2608\chi_{16} + 0.0008\chi_{17}$

$\phi_{15} = 0.0003\chi_2 - 0.0030\chi_3 + 1.0226\chi_4 - 0.0001\chi_{11} + 0.0008\chi_{12} - 0.2618\chi_{13} - 0.0001\chi_{15} + 0.0008\chi_{16} - 0.2618\chi_{17}$

$\phi_{16} = -1.1220\chi_1 - 0.0001\chi_2 - 0.4012\chi_5 + 0.2352\chi_6 - 0.0703\chi_7 + 0.3731\chi_{10} - 0.6063\chi_{11} - 0.0527\chi_{12} + 0.3730\chi_{14} + 0.6062\chi_{15} + 0.0527\chi_{16}$

$\phi_{17} = 0.0001\chi_1 - 1.4504\chi_2 - 0.1261\chi_3 + 0.5300\chi_{10} - 0.6493\chi_{11} - 0.0565\chi_{12} - 0.5301\chi_{14} - 0.6494\chi_{15} - 0.0565\chi_{16}$

### 3.2 Ruthenium dibromide

Ruthenium(II) bromideis also triatomic molecule, having the following optimized geometry as obtained from molecular mechanics method.

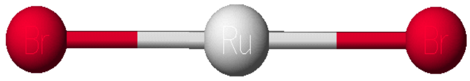

Bond Length=2.389Å

Bond Angle=179.99$^0$

**Fig. 2 Structure of $RuBr_2$**

The MOs of this molecule as formed by linear combination of 17AOs ($\chi_1$-$\chi_{17}$), where $\chi_1$ = 5s, $\chi_2$ = 5px, $\chi_3$ = 5py, $\chi_4$ = 5pz, $\chi_5$ = 4dx$^2$-y$^2$, $\chi_6$ = 4dz$^2$, $\chi_7$ = 4dxy, $\chi_8$ = 4dxz, $\chi_9$ = 4dyz, for Ru-1 and $\chi_{10}$ = 4s, $\chi_{11}$ = 4px, $\chi_{12}$ = 4py, $\chi_{13}$ = 4pz for Br-2 and $\chi_{14}$ = 4s, $\chi_{15}$ = 4px, $\chi_{16}$ = 4py, $\chi_{17}$ = 4pz for Br-3. The 17 AOs on LCAO approximations give 17 MOs($\phi_1$–$\phi_{17}$). The magnitude of contribution of various 17 $\chi$s in the formation of 17 $\phi$s, is demonstrated by Eqs., $\phi_1$ to $\phi_{17}$. Here, the coefficients of $\chi$ are the eigenvector and its zero or near zero values have been omitted.

$\phi_1 = 0.1235\chi_1 + 0.1404\chi_5 - 0.0823\chi_6 + 0.0246\chi_7 + 0.6531\chi_{10} + 0.0020\chi_{11} + 0.0002\chi_{12} + 0.6531\chi_{14} - 0.0020\chi_{15} - 0.0002\chi_{16}$

$\phi_2 = -0.0869\chi_2 - 0.0076\chi_3 - 0.6794\chi_{10} - 0.0174\chi_{11} - 0.0015\chi_{12} + 0.6794\chi_{14} - 0.0174\chi_{15} - 0.0015\chi_{16}$

$\phi_3 = 0.0412\chi_1 + 0.5894\chi_5 - 0.3455\chi_6 + 0.1033\chi_7 - 0.1904\chi_{10} - 0.4010\chi_{11} - 0.0349\chi_{12} - 0.1904\chi_{14} + 0.4010\chi_{15} + 0.0349\chi_{16}$

$\phi_4 = -0.0001\chi_7 - 0.8827\chi_8 - 0.0768\chi_9 - 0.2694\chi_{13} + 0.2694\chi_{17}$

$\phi_5 = 0.1529\chi_5 - 0.8728\chi_7 + 0.0001\chi_8 + 0.0233\chi_{11} - 0.2683\chi_{12} - 0.0233\chi_{15} + 0.2683\chi_{16}$

$\phi_6 = -0.0866\chi_8 + 0.9962\chi_9$

$\phi_7 = 0.4925\chi_5 + 0.8660\chi_6 + 0.0863\chi_7$

$\phi_8 = 0.1943\chi_2 + 0.0169\chi_3\ 0.0796\chi_{10} - 0.6248\chi_{11} - 0.0543\chi_{12} + 0.0796\chi_{14} - 0.6248\chi_{15} - 0.0543\chi_{16}$

$\phi_9 = 0.0109\chi_2 - 0.1249\chi_3 + 0.0593\chi_{11} - 0.6820\chi_{12} - 0.6820\chi_{15} - 0.6820\chi_{16}$

$\phi_{10} = 0.1254\chi_4 + 0.6846\chi_{13} + 0.6846\chi_{17}$

$\phi_{11} = -0.4988\chi_1 + 0.5413\chi_5 - 0.3173\chi_6 + 0.0949\chi_7 + 0.0328\chi_{10} + 0.3692\chi_{11} + 0.0321\chi_{12} + 0.0328\chi_{14} - 0.3692\chi_{15} - 0.0321\chi_{16}$

$\phi_{12} = 0.0002\chi_5 - 0.0009\chi_7 - 0.4733\chi_8 - 0.0412\chi_9 - 0.0001\chi_{11} + 0.0012\chi_{12} + 0.6580\chi_{13} + 0.0001\chi_{15} - 0.0012\chi_{16} - 0.6580\chi_{17}$

$\phi_{13} = -0.0820\chi_5 + 0.4679\chi_7 - 0.0009\chi_8 - 0.0001\chi_9 + 0.0570\chi_{11} - 0.6556\chi_{12} + 0.0012\chi_{13} - 0.0570\chi_{15} + 0.6556\chi_{16}\ 0.0012\chi_{17}$

$\phi_{14} = 0.0876\chi_2 - 1.0075\chi_3 - 0.0041\chi_4 - 0.0195\chi_{11} + 0.2238\chi_{12} + 0.0009\chi_{13} - 0.0195\chi_{15} + 0.2238\chi_{16} + 0.0009\chi_{17}$

$\phi_{15} = -0.0004\chi_2 + 0.0041\chi_3 - 1.0113\chi_4 + 0.0001\chi_{11} - 0.0009\chi_{12} + 0.2246\chi_{13} + 0.0001\chi_{15} - 0.0009\chi_{16} + 0.2246\chi_{17}$

$\phi_{16} = 1.0382\chi_1 + 0.3628\chi_5 - 0.2127\chi_6 + 0.0636\chi_7 - 0.3224\chi_{10} + 0.5860\chi_{11} + 0.0510\chi_{12} - 0.3224\chi_{14} - 0.5860\chi_{15} - 0.0510\chi_{16}$

$\phi_{17} = 1.3428\chi_2 + 0.1168\chi_3 - 0.4462\chi_{10} + 0.6090\chi_{11} + 0.0530\chi_{12} + 0.4462\chi_{14} + 0.6090\chi_{15} + 0.0530\chi_{16}$

### 3.3 Ruthenium diiodide

The optimized geometry of $RuI_2$ as obtained from molecular mechanics method is shown below.

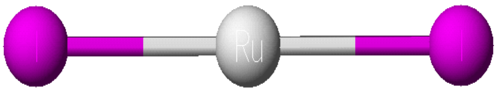

Bond Length = 2.579Å

Bond Angle=179.99$^0$

**Fig. 3 Structure of $RuI_2$**

The MOs of this molecule is formed by linear combination of 17AOs ($\chi_1$-$\chi_{17}$), where $\chi_1$ = 5s, $\chi_2$ = 5px, $\chi_3$ = 5py, $\chi_4$ = 5pz, $\chi_5$ = 4dx2-y2, $\chi_6$ = 4dz2, $\chi_7$ = 4dxy, $\chi_8$ = 4dxz, $\chi_9$ = 4dyz, for Ru-1 and $\chi_{10}$ = 5s, $\chi_{11}$ = 5px, $\chi_{12}$ = 5py, $\chi_{13}$ = 5pz for I-2 and $\chi_{14}$ = 5s, $\chi_{15}$ = 5px, $\chi_{16}$ = 5py, $\chi_{17}$ = 5pz for I-3).The magnitude of contribution of various AOs ($\chi_1$–$\chi_{17}$) in the formation of 17 MOs is demonstrated by Eqs., $\phi_1$ to $\phi_{17}$as given below. Here, the coefficients of $\chi$ are the eigenvector and its zero or near zero values have been omitted.

$$\phi_1 = 0.1682\chi_1+0.2485\chi_5-0.1457\chi_6+0.0436\chi_7+0.6041\chi_{10}-0.0468\chi_{11}-0.0041\chi_{12}+0.6045\chi_{14}+0.0468\chi_{15}+0.0041\chi_{16}$$

$$\phi_2 = -0.1185\chi_2 -0.0103\chi_3 -0.6705\chi_{10} -0.0091\chi_{11} -0.0008\chi_{12} +0.6700\chi_{14} -0.0091\chi_{15} -0.0008\chi_{16}$$

$$\phi_3 = -0.0001\chi_5 +0.0003\chi_7 +0.9276\chi_8 +0.0807\chi_9 +0.0001\chi_{12} +0.2075\chi_{13} -0.0001\chi_{16} -0.2077\chi_{17}$$

$$\phi_4 = -0.1607\chi_5 +0.9172\chi_7 -0.0003\chi_8 -0.0180\chi_{11} +0.2068\chi_{12} -0.0001\chi_{13} +0.0180\chi_{15} -0.2069\chi_{16} +0.0001\chi_{17}$$

$$\phi_5 = 0.0083\chi_1 -0.6139\chi_5 +0.3598\chi_6 -0.1076\chi_7 +0.2911\chi_{10} +0.3522\chi_{11} +0.0306\chi_{12} +0.2912\chi_{14} -0.3523\chi_{15} -0.0306\chi_{16}$$

$$\phi_6 = 0.0866\chi_8 -0.9962\chi_9$$

$$\phi_7 = -0.4925\chi_5 -0.8660\chi_6 -0.0863\chi_7$$

$$\phi_8 = -0.0003\chi_1 +0.2094\chi_2 +0.0182\chi_3 +0.0182\chi_5 -0.0002\chi_6 -0.1031\chi_{10} -0.6166\chi_{11} -0.0536\chi_{12} +0.1032\chi_{14} -0.6169\chi_{15} -0.0536\chi_{16}$$

$$\phi_9 = -0.4974\chi_1 -0.0001\chi_2 +0.4844\chi_5 -0.2839\chi_6 +0.0849\chi_7 +0.0636\chi_{10} +0.4048\chi_{11} +0.0352\chi_{12} +0.0635\chi_{14} -0.4041\chi_{15} -0.0351\chi_{16}$$

$$\phi_{10} = 0.0002\chi_2 -0.0024\chi_3 +0.1194\chi_4 +0.0012\chi_{11} -0.0138\chi_{12} +0.6880\chi_{13} +0.0012\chi_{15} -0.0138\chi_{16} +0.6877\chi_{17}$$

$$\phi_{11} = -0.0103\chi_2 +0.1189\chi_3 +0.0024\chi_4 -0.0596\chi_{11} +0.6854\chi_{12} +0.0139\chi_{13} -0.0596\chi_{15} +0.6851\chi_{16} +0.0139\chi_{17}$$

$$\phi_{12} = -0.0001\chi_4 -0.0001\chi_5 +0.0005\chi_7 -0.3732\chi_8 -0.0325\chi_9 +0.0001\chi_{11} -0.0009\chi_{12} +0.6786\chi_{13} -0.0001\chi_{15} +0.0009\chi_{16} -0.6789\chi_{17}$$

$$\phi_{13} = -0.0001\chi_3 +0.0647\chi_5 -0.3690\chi_7 -0.0005\chi_8 -0.0588\chi_{11} +0.6760\chi_{12} +0.0009\chi_{13} +\chi_{14} +0.0588\chi_{15} -0.6763\chi_{16} -0.0009\chi_{17}$$

$$\phi_{14} = 0.0004\chi_2 -0.0040\chi_3 -1.0073\chi_4 -1.0073\chi_{11} +0.0008\chi_{12} +0.2026\chi_{13} -0.0001\chi_{15} +0.0008\chi_{16} +0.2027\chi_{17}$$

$$\phi_{15} = -0.0873\chi_2 +1.0035\chi_3 -0.0040\chi_4 +0.0175\chi_{11} -0.2018\chi_{12} +0.0008\chi_{13} +0.0176\chi_{15} -0.2019\chi_{16} +0.0008\chi_{17}$$

$$\phi_{16} = -1.0160\chi_1 -0.0008\chi_2 -0.0001\chi_3 -0.3238\chi_5 +0.1898\chi_6 -0.0568\chi_7 +0.3211\chi_{10} -0.5795\chi_{11} -0.0504\chi_{12} +0.3207\chi_{14} +0.5789\chi_{15} +0.0503\chi_{16}$$

$$\phi_{17} = -0.0008\chi_1 +1.3012\chi_2 +0.1131\chi_3 -0.0003\chi_5 +0.0002\chi_6 -0.0001\chi_7 -0.4205\chi_{10} +0.6005\chi_{11} +0.0522\chi_{12} +0.4212\chi_{14} +0.6014\chi_{15} +0.0523\chi_{16}$$

The characteristics of transition metal (TM) elements are due to their d orbitals of (n-1) shell and s and p orbitals of n shell. As the atom of TM elements form compound they adopted either concept of bonded attraction and non-bonded repulsion of VB (Valence Bond) theory, and or positive and negative overlap populations of MO (Molecular Orbital) theory [3-5]. In the first case they may undergo various type of hybridization that depends upon the oxidation state of TM and number and nature of combing atoms or ions, and in the second case formation of molecular orbital by LCAO approximation [6].

At first we have to examine the extent of involvement of 4d, 5s and 5p AOs of Ru-1 in the formation of MOs in ruthenium dihalides. To see the total involvement of seven AOs of Ru-1 in eleven MOs ($\phi_1$-$\phi_{11}$), the coefficient value ($c_i$) of each orbital ($\chi_i$) has been added. The $\chi$ of non-bonding orbitals 4dz2 ($\chi_6$) and 4dyz ($\chi_9$) are excluded. The six vacant MOs ($\phi_{12}$-$\phi_{17}$) are exempted here, as there is only 22e$^-$ to be filled by following Aufbau principle, Hund's rule and Pauli's exclusion principle and thus we considered only eleven MOs among seventeen MOs.

| ΣAO | $RuCl_2$ | $RuBr_2$ | $RuI_2$ |
|---|---|---|---|
| Σ4dx$^2$-y$^2$ | 1.8387 | 1.9165 | 2.0004 |
| Σ4dxy | 1.0407 | 1.1820 | 1.2399 |
| Σ4dxz | 0.8364 | 0.9694 | 1.0145 |
| Σ5s | 0.6598 | 0.6635 | 0.6742 |
| Σ5px | 0.2471 | 0.2921 | 0.3385 |
| Σ5py | 0.1477 | 0.1494 | 0.1498 |
| Σ5pz | 0.1276 | 0.1254 | 0.1218 |

The summation values of AOs in these eleven MOs as given above, clearly reflects maximum nvolvement is of 4d orbital (4dx$^2$-y$^2$> 4dxz > 4dxy). Next to this is 5s orbital. The involvements of three p-orbitals are negligible as their summation value is very low in comparison to d orbital and considerably low with respect to s orbital. It is also evident from these data that the involvement of 5p orbital in Ru—X bond is insignificant and the main role is played by 5s and by 4d orbital. Landis has also force fully deprived of the involvement of np orbital in hybridization in transition metals and supported sd$^n$ hybridization (here n = 1) [7]. He has also described the hybridization bond angle and idealized molecular shapes for sd$^n$-hybridization and plotted graph between energy and bond angle.

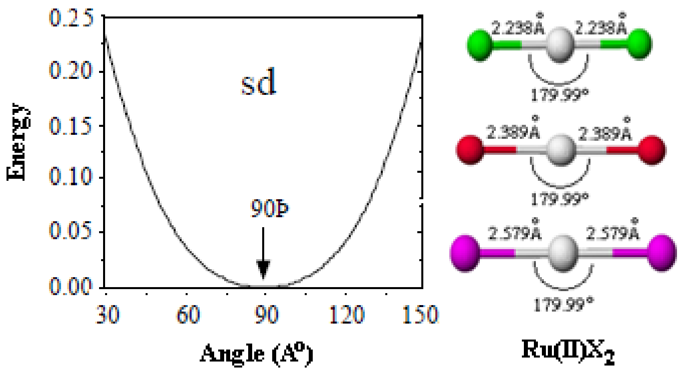

**Fig.4 Plot between energy and bond angle(Å) for sd-hybridization**

As can be seen from figure 4 that bond angle (as presented by Landis et al.) has two minima one below 90° and one above 90°. This is because the energy curves are a function of the bond angles. The bond angles as presented in figure also hold up the Landis model of sd$^n$-hybridization, when n=1. Landis recommended that transition metals in their valency shell can accommodate only 12 electrons, 10e$^-$ in five (n-1)d orbitals and 2e$^-$ in one ns-orbital. The 18 electrons can be in their valency shell, 10e$^-$ in five (n-1)d orbitals, 2e$^-$ in one ns-orbital and 6e$^-$ in three np orbitals, if they have their participation. Further, a close look at the bottom right side in the figures, 5-7, these very clearly demonstrated that the summation values are highest in case of iodide and lowest in chloride. This is due to cloud expending of halides. For a given metal ion, the ability of ligands to induce this cloud expending increases according to nephelauxetic series: $F^- < H_2O < NH_3 < en < ox < SCN < Cl^- < CN^- < Br^- < I^-$[8]. Thus, iodide produces greater cloud expending effect than bromide, which intern produces higher than chloride in ruthenium diiodide, ruthenium dibromide and ruthenium dichloride, respectively. In orther words, the effective positive charge on Ru(II) is reduced greater by iodide and lesser by chloride. The result is in good agreement with nephelauxetic series of ligands. This effect can also be related with the difference in energy levels of ns and np orbitals of the halogens. Halogens enter into bonding through their s and p orbitals. These two orbitals differ in energy significantly. The energy difference Δε in s and p orbitals of the chloride, bromide and iodide are not same.

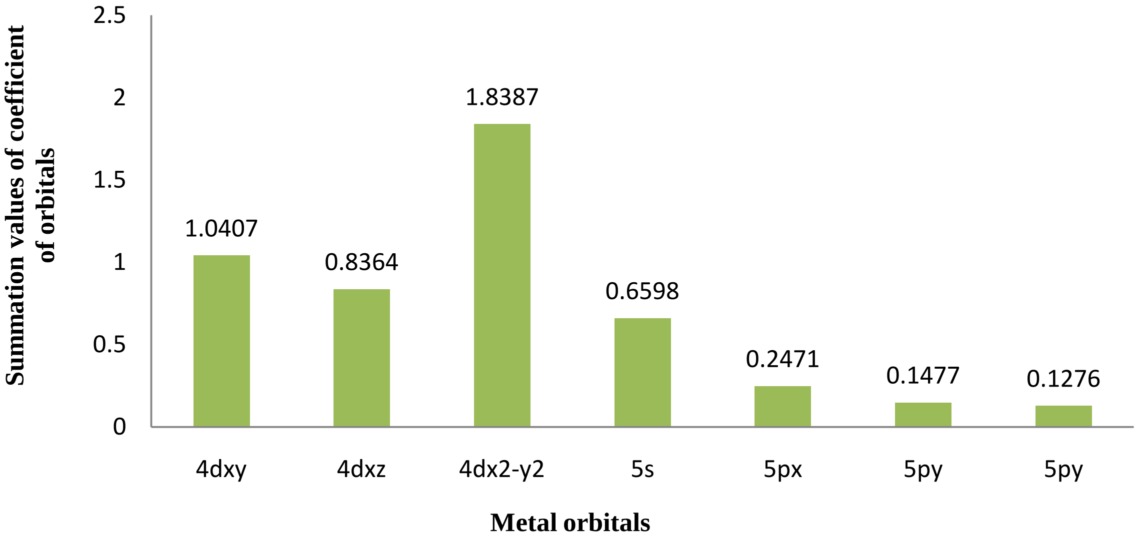

**Fig. 5 Extent of involvement of metal orbital in the formation of MOs of RuCl$_2$**

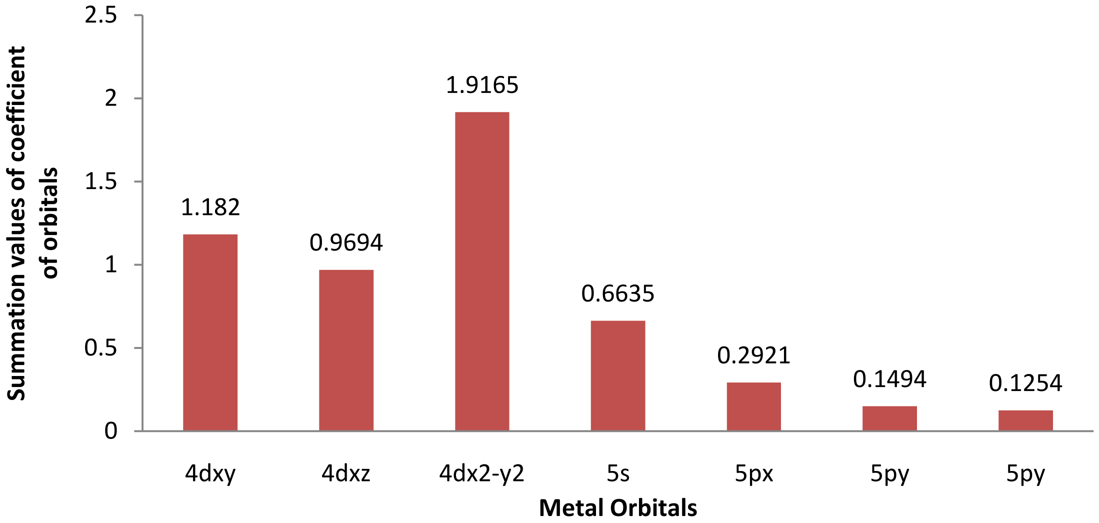

**Fig. 6 Extent of involvement of metal orbital in the formation of MOs of $RuBr_2$.**

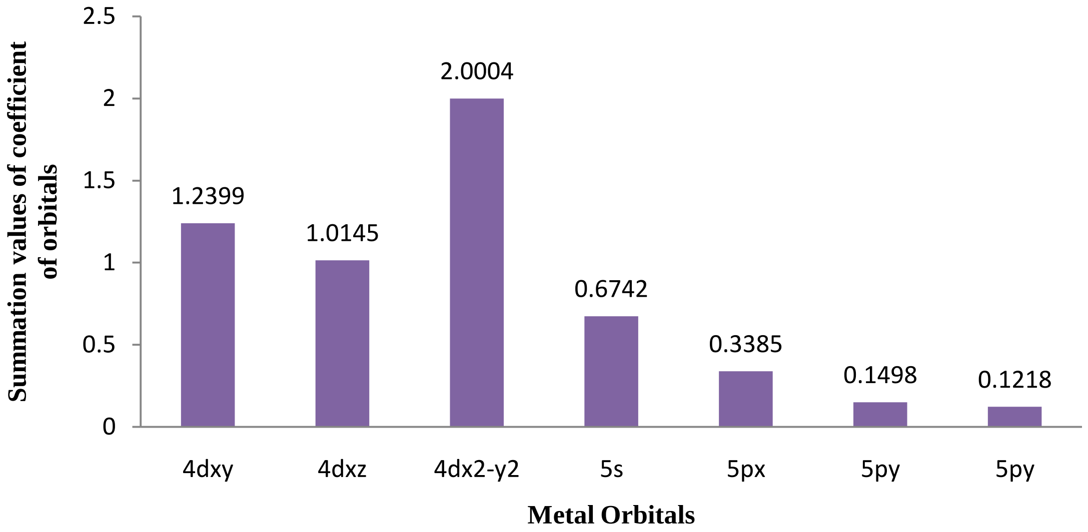

**Fig. 7 Extent of involvement of metal orbital in the formation of MOs of $RuI_2$.**

The s and p orbitals in iodide are close as compared to s and p orbitals of bromide and chloride, as shown below.

| **Energy (eV)** | **Cl** | **Br** | **I** |
|---|---|---|---|
| $\varepsilon_s$ | -0.9665 | -0.8110 | -0.6615 |
| $\varepsilon_p$ | -0.5218 | -0.4814 | -0.4867 |
| $\Delta\varepsilon_{s-p}$ | -0.4447 | -0.3296 | -0.2148 |

Iodide, in which s and p orbitals are much close causes greater nephelauxetic effect and thus increases the covalent bond character in the molecule.Percentage of ionic and covalent bond character of $Ru(II)Cl_2$, $Ru(II)Br_2$ and $Ru(II)I_2$ has beencalculated by solving equation “% ionic character=$16\times\Delta\chi+3.5\times(\Delta\chi)^2$”, and results are shown below:

| **Compound** | **$RuCl_2$** | **$RuBr_2$** | **$RuI_2$** |
|---|---|---|---|
| % Ionic Character | 24.240 | 5.115 | 3.340 |
| % Covalent Character | 75.760 | 94.885 | 96.660 |

The result is in good agreement with experiment results that covalent character increases in the order: $RuI_2 > RuBr_2 > RuCl_2$.

**Table-1.** Overlaps between the various AOs of constituents atom in each MO

| NO | AO—AO | NO | AO—AO |
|---|---|---|---|
| 1 | (Ru-1)5s—ns(X-2) | 45 | (Ru-1)4dz$^2$—ns(X-3) |
| 2 | (Ru-1)5s—npx(X-2) | 46 | (Ru-1)4dz$^2$—npx(X-3) |
| 3 | (Ru-1)5s—npy(X-2) | 47 | (Ru-1)4dz$^2$—npy(X-3) |
| 4 | (Ru-1)5s—npz(X-2) | 48 | (Ru-1)4dz$^2$—npz(X-3) |
| 5 | (Ru-1)5s—ns(X-3) | 49 | (Ru-1)4dxy—ns (X-2) |
| 6 | (Ru-1)5s—npx(X-3) | 50 | (Ru-1) 4dxy—npx (X-2) |
| 7 | (Ru-1)5s—npy(X-3) | 51 | (Ru-1)4dxy—npy(X-2) |
| 8 | (Ru-1)5s—npz(X-3) | 52 | (Ru-1)4dxy—npz(X-2) |
| 9 | (Ru-1)5px—ns(X-2) | 53 | (Ru-1)4dxy—ns(X-3) |
| 10 | (Ru-1)5px—npx(X-2) | 54 | (Ru-1)4dxy—npx(X-3) |
| 11 | (Ru-1)5px—npy (X-2) | 55 | (Ru-1)4dxy—npy(X-3) |
| 12 | (Ru-1)5px—npz (X-2) | 56 | (Ru-1)4dxy—npz(X-3) |
| 13 | (Ru-1)5px—ns (X-3) | 57 | (Ru-1)4dxz—ns(X-2) |
| 14 | (Ru-1)5px—npx(X-3) | 58 | (Ru-1)4dxz—npx(X-2) |
| 15 | (Ru-1)5px—npy(X-3) | 59 | (Ru-1)4dxz—npy(X-2) |
| 16 | (Ru-1)5px—npz(X-3) | 60 | (Ru-1)4dxz—npz(X-2) |
| 17 | (Ru-1)5py—ns(X-2) | 61 | (Ru-1)4dxz—ns(X-3) |
| 18 | (Ru-1)5py—npx(X-2) | 62 | (Ru-1)4dxz—npx(X-3) |
| 19 | (Ru-1)5py—npy(X-2) | 63 | (Ru-1)4dxz—npy(X-3) |
| 20 | (Ru-1)5py—npz(X-2) | 64 | (Ru-1)4dxz—npz(X-3) |
| 21 | (Ru-1)5py—ns(X-3) | 65 | (Ru-1)4dyz—ns(X-2) |
| 22 | (Ru-1)5py—npx(X-3) | 66 | (Ru-1)4dyz—npx(X-2) |
| 23 | (Ru-1)5py—npy(X-3) | 67 | (Ru-1)4dyz—npy(X-2) |
| 24 | (Ru-1)5py—npz(X-3) | 68 | (Ru-1)4dyz—npz(X-2) |
| 25 | (Ru-1)5pz—ns(X-2) | 69 | (Ru-1)4dyz—ns(X-3) |
| 26 | (Ru-1)5pz—npx(X-2) | 70 | (Ru-1)4dyz—npx(X-3) |
| 27 | (Ru-1)5pz—npy(X-2) | 71 | (Ru-1)4dyz—npy(X-3) |
| 28 | (Ru-1)5pz—npz(X-2) | 72 | (Ru-1)4dyz—npz(X-3) |
| 29 | (Ru-1)5pz—ns(X-3) | 73 | (X-2)ns—ns(X-3) |
| 30 | (Ru-1)5pz—npx(X-3) | 74 | (X-2)ns—npx(X-3) |
| 31 | (Ru-1)5pz—npy (X-3) | 75 | (X-2)ns—npy(X-3) |
| 32 | (Ru-1)5pz—npz(X-3) | 76 | (X-2)ns—npz(X-3) |
| 33 | (Ru-1)4dx$^2$-y$^2$—ns(X-2) | 77 | (X-2)npx—ns(X-3) |
| 34 | (Ru-1)4dx$^2$-y$^2$—npx(X-2) | 78 | (X-2)npx—npx(X-3) |
| 35 | (Ru-1)4dx$^2$-y$^2$—npy(X-2) | 79 | (X-2)npx—npy(X-3) |
| 36 | (Ru-1)4dx$^2$-y$^2$—npz(X-2) | 80 | (X-2)npx—npz(X-3) |
| 37 | (Ru-1)4dx$^2$-y$^2$—ns(X-3) | 81 | (X-2)npy—ns(X-3) |
| 38 | (Ru-1)4dx$^2$-y$^2$—npx(X-3) | 82 | (X-2)npy—npx(X-3) |
| 39 | (Ru-1)4dx$^2$-y$^2$—npy(X-3) | 83 | (X-2)npy—npy(X-3) |
| 40 | (Ru-1)4dx$^2$-y$^2$—npz(X-3) | 84 | (X-2)npy—npz(X-3) |
| 41 | (Ru-1)4dz$^2$—ns(X-2) | 85 | (X-2)npz—ns( X-3) |
| 42 | (Ru-1)4dz$^2$—npx(X-2) | 86 | (X-2)npz—npx(X-3) |
| 43 | (Ru-1)4dz$^2$—npy(X-2) | 87 | (X-2)npz—npy(X-3) |
| 44 | (Ru-1)4dz$^2$—npz(X-2) | 88 | (X-2)npz—npz(X-3) |

where, X = Cl, Br, I, and n = 3 for Cl, n = 4 for Br and n = 5 for I.

Mulliken population analysis method [2] has been used to measure the contribution of electrons in each occupied MO. For this Eq.2 has been solved for 22e$^-$ by putting 2e$^-$ in each MO ($\phi_1$-$\phi_{11}$).The shape of each MO($\phi_1$-$\phi_{17}$) has been determined by the relative magnitudes and signs of the different coefficients. For this the $RuX_2$ has been decomposed into three parts: Ru-1, X-1 and X-2, and the MO of the complete system has been obtained by allowing the orbitals of Ru-1 (4d, 5s, 5p), X-1 (ns and np) and X-2 (ns and np) to overlap. The possible overlaps between the various AOs of ruthenium (Ru-1) and halogens (X-2 and X-2) in each MO will be 88, as describes in Table-1. The number of electrons is taken as two for $\phi_1$ to $\phi_{11}$ and zero for $\phi_{12}$ to $\phi_{17}$. Finally, Eq.3 has been solved for these eleven MOs with respect to each halide. In order to get a precise description, the sum of overlap populations for the eleven MOs of $RuCl_2$, $RuBr_2$ and $RuI_2$ have been worked out and results are presented in table 1-3, respectively.

**Table-2. Nature of occupied molecular orbitals of $RuCl_2$**

| MO No. | $\Sigma n_{r-s,i}$ | sign | Nature of MOs |
|---|---|---|---|
| 1 | 0.1924 | (Positive) | Bonding |
| 2 | 0.1237 | (Positive) | Bonding |
| 3 | 0.4502 | (Positive) | Bonding |
| 4 | 0.2226 | (Positive) | Bonding |
| 5 | 0.2228 | (Positive) | Bonding |
| 6 | 0.0000 | (zero) | Nonbonding |
| 7 | 0.0000 | (zero) | Nonbonding |
| 8 | 0.2853 | (Positive) | Bonding |
| 9 | 0.1182 | (Positive) | Bonding |
| 10 | 0.1202 | (Positive) | Bonding |
| 11 | 0.0735 | (Positive) | Bonding |

**Table-3. Nature of occupied molecular orbitals of $RuBr_2$**

| MO No. | $\Sigma n_{r-s,i}$ | sign | Nature of MOs |
|---|---|---|---|
| 1 | 0.2091 | (Positive) | Bonding |
| 2 | 0.1371 | (Positive) | Bonding |
| 3 | 0.2487 | (Positive) | Bonding |
| 4 | 0.1395 | (Positive) | Bonding |
| 5 | 0.1395 | (Positive) | Bonding |
| 6 | 0.0000 | (zero) | Nonbonding |
| 7 | 0.0000 | (zero) | Nonbonding |
| 8 | 0.3256 | (Positive) | Bonding |
| 9 | 0.0941 | (Positive) | Bonding |
| 10 | 0.0940 | (Positive) | Bonding |
| 11 | 0.1433 | (Positive) | Bonding |

**Table-4. Nature of occupied molecular orbitals of $RuI_2$**

| MO No. | $\Sigma n_{r-s,i}$ | sign | Nature of MOs |
|---|---|---|---|
| 1 | 0.3042 | (Positive) | Bonding |
| 2 | 0.1742 | (Positive) | Bonding |
| 3 | 0.0936 | (Positive) | Bonding |
| 4 | 0.0936 | (Positive) | Bonding |
| 5 | 0.1248 | (Positive) | Bonding |
| 6 | 0.0000 | (zero) | Nonbonding |
| 7 | 0.0000 | (zero) | Nonbonding |
| 8 | 0.3359 | (Positive) | Bonding |
| 9 | 0.1849 | (Positive) | Bonding |
| 10 | 0.0783 | (Positive) | Bonding |
| 11 | 0.0783 | (Positive) | Bonding |

As can be seen from Table-2 that among the eleven molecular orbital, nine are bonding and two are nonbonding. The bonding molecular orbitals are$\phi_1$–$\phi_5$and $\phi_8$–$\phi_{11}$. The nonbonding molecular orbital are $\phi_6$ and$\phi_7$, which are purely two d atomic orbitals of ruthenium namely dxz and $dz^2$. Table-3 shows that among the eleven molecular orbital of $RuBr_2$, nine are bonding and two are nonbonding. The bonding molecular orbitals are $\phi_1$–$\phi_5$and $\phi_8$–$\phi_{11}$. The nonbonding molecular orbital are $\phi_6$ and$\phi_7$, which are purely two d atomic orbitals of ruthenium namely dxz and $dz^2$. Table-4 shows that among the eleven molecular orbital of $RuI_2$, nine are bonding and two are nonbonding. The bonding molecular orbitals are $\phi_1$–$\phi_5$and $\phi_8$–$\phi_{11}$. The nonbonding molecular orbital are $\phi_6$ and$\phi_7$, which are purely two d atomic orbitals of ruthenium namely dxz and $dz^2$. A comparative study of table 2 to 4 reflected that in all cases the nonbonding electrons are present in 6th and 7th molecular orbitals. Further, similarity in positions of nonbonding molecular orbitals prompted us to examine the eigenvalues of $Ru^{+2}$ion and to compare them with the eigenvalues of the halides.

**Scheme-1. Splitting of d orbitals in Ruthenium(II) halides**

| **Energy (eV)** | **Ru++** | **$RuCl_2$** | **$RuBr_2$** | **$RuI_2$** |
|---|---|---|---|---|
| -0.4521 | | 4dxz, 4dxy | | |
| -0.4579 | | | 4dxy, 4dxz | |
| -0.4725 | | | | 4dxy, 4dxz |
| -0.5476 | $4dx^2$-$y^2$, $4dz^2$, 4dxy, 4dyz, 4dxz | 4dyz, $4dz^2$ | 4dyz, $4dz^2$ | 4dyz, $4dz^2$ |
| -0.5560 | | | | $4dx^2$-$y^2$ |
| -0.5702 | | | $4dx^2$-$y^2$ | |
| -0.5934 | | $4dx^2$-$y^2$ | | |

The energies of atomic orbitals of $Ru^{+2}$ion, and in its three halides are demonstrated in scheme 2, which shows that all the d orbitals in $Ru^{+2}$ion are degenerate and their energy is –0.5476eV. The energy of 4dyz, and $4dz^2$ orbitals (–0.5476 eV) in all the halides are also same, which confirmed non-bonding MOs are these pure d-AOs of Ru-1. In case of chloride the energy of $4dx^2$–$y^2$is -0.5934eV and in bromide and iodide, –0.5702eV and –0.5560eV respectively. The 4dxy, and 4dxz are degenerate in all the cases but their energies differ, being –4521eV in chloride, –0.4579eV in bromide and –0.4725eV in iodide. The energy separation $\Delta E^-$ between the energy levels of the nonbonding and antibonding MO is directly link to the strength of the interaction between the ligand orbitals and those on metal. The stronger this interaction, the more the antibonding orbitals are destabilized, so the larger the energy gap $\Delta E^-$. The magnitude of splitting of metal d orbital has also been studiedbycalculatingenergy separationof nonbonding degenerate orbitals(4dyz, $4dz^2$) and $4dx^2$-$y^2$ or 4dxy, 4dxz. The highest value is in chloride and lowest in iodide and as shown by Scheme-2. This is in agreement with spectrochemical series of ligands [9].

## IV. CONCLUSION

(i) The $\sum c_i$values of AOs of Ru-metal in their halides ($RuCl_2$, $RuBr_2$, and $RuI_2$) show sd-hybridization, which is supported by their bond angles as proposed by Landis et al.

(ii) Further, summation values follow the trend $RuI_2 > RuBr_2 > RuCl_2$, which shows good agreement with nephelauxetic series of ligands.

(iii) The magnitude of splitting of $Ru^{2+}$ d-orbitals follow the trend $RuCl_2 > RuBr_2 > RuI_2$, which is in good agreement with spectrochemical series of ligands.

(iv) Population analysis study shows among the seventeen ($\phi_1-\phi_{17}$) MOs formed by LCAO-MO approximation, nine ($\phi_1-\phi_5$ and $\phi_8-\phi_{11}$) are bonding, two ($\phi_6$ and $\phi_7$) are nonbonding and remaining six ($\phi_{12}-\phi_{17}$) are antibonding. The nonbonding MOs, $\phi_6$ and $\phi_7$, are purely 4dyx and $4dz^2$ AOs of ruthenium, respectively.

(v) MOTclearly demonstrates the energy levels of different molecular orbitals, the position of nonbonding MOs and energy gap $\Delta E^-$ and $\Delta E^+$ due to splitting. Further, MO diagram reflected that all the MOs ($\phi_1-\phi_{17}$) have definite energy and definite shape due to (a) different contribution ( $c_{ri}$ and $c_{si}$ ) of many basis functions ($\chi_1-\chi_{17}$) (b) difference in energies ($\Delta\varepsilon$) of overlaping AOs (c) difference in overlap integral ($S_{r-s}$) and (d) symmetry (phase) of overlapping AOs. And, thus provide clear cut electronic picture of the molecule, which more precisely explain or help to explain the various properties of the molecule.

## ACKNOWLEDGEMENTS

The authors are thankful to Principal, M.L.K. (P.G.) College, Balrampur (U.P.), India for laboratory facilities.

## REFERENCES

[1]. (a) Singh, R.K, Sharma, P.D. and Singh, P. P., "Molecular Mechanics Based Study of Molecular Orbital of Cobalt(II) halides." *Asian J. Chem*. 2007; 19(1), 121.(b) Khan, G. and Tewari, R.P., "Study of Molecular Orbitals of Ruthenium (II) Bromide Based on Molecular Mechanics," Arch. Appl. Sci. Res. 2011; 3(2), 483. (c) Khan, G., Verma, R. N. and Pandey, B.P.Study of Molecular Orbitals of Ruthenium (II) Bromide Based on Molecular Mechanics," J. Chem. Pharm. Res. 2011; 3(2), 172. (d) Khan, G., Shukla, A. and Tewari, R.P., "Comparative Study of Molecular Orbitals of Ruthenium (II) Bromide and Ruthenium (II) Iodide on Molecular Mechanics," Int.J. ChemTech Res. 2012; 4(1), 445.

[2]. (a) Mulliken, R.S., "Electronic Population Analysis on LCAO-MO Molecular Wave Function.I." *J. Chem. Phys.* 1955; 23, 1833. (b) Mulliken, R.S., "Electronic Population Analysis on LCAO-MO Molecular Wave Function.II. Overlap Populations, Bond Order, and Covalent Bond Energies," *J. Chem. Phys.* 1955; 23, 1841. (c) Mulliken, R.S., "Electronic Population Analysis on LCAO-MO Molecular Wave Function.III. Efffects of Hybridization on Overlap and Gross AO Populations" *J. Chem. Phys.* 1955; 23, 2338. (d) Mulliken, R.S., "Electronic Population Analysis on LCAO-MO Molecular Wave Function.IV. Bonding and Antibonding in LCAO and Valence-Bond Theories" *J. Chem. Phys.* 1955; 23, 2343.

[3]. Heitler, W. and London, F., "WechselwirkungneutralerAtome und homoopolare Binding nach der Quantenmechanik" *Z. Physik.* 1927; 44, 455.

[4]. Pauling, L. and Wilson, E.B., "Introduction to Quantum Mechanics," McGraw-Hill Book Company, Inc. New York, 1935, pp340-380.

[5]. Water, E. and Kimball, "Quantum Chemistry," John Wiley and Sons, Inc., New York, 1944.

[6]. (a) Pople, J. A. Santry, D. P. and Segal, G. A., "Approximate Self-Consistent Molecular Orbital Theory I. Invariant Procedures." *J. Chem. Phys.* 1965, *43*, 5129. (b) Pople, J. A. and Segal, G. A., "Approximate Self-Consistent Molecular Orbital Theory II. Calculations with Complete Neglect of Differential Overlap," *J. Chem. Phys.*1966, *44*, 3289.

[7]. (a) Landis, C. R., Lipkowitz, K. B. and Boyd, D. B. *Reviews in Computational Chemistry*, Vol. 6, VCH, 1995, Chapter 2. (b) Landis, C. R., Cleveland, T. and Firman, T. K., "Making sence of the shape of simple metal hydrides," *J. Am. Chem. Soc.*1995, *117*, 1859. (c) Landis, C. R., Firman, T. K., Root, D.M. and Cleveland, T., "A valence bond perspective on the molecular shapes of simple metal alkyls and hydrides.," *J. Am. Chem. Soc.* 1998, *120*, 1842. (d) Landis, C. R., Cleveland, T. and Firman, T. K., "Valence bond concepts applied to the molecular mechanics description of molecular shapes.3. Applications to transition metal alkyls and hydrides," *J. Am. Chem. Soc.*1998, *120*, 2641.

[8]. Tchougreeff, A. L. and Dronskowski, R., "Nephelauxetic Effect Revisited," *Int. J. Quan. Chem.* 2009; 109, 2606.

[9]. Fielder, S.S., Osborne, Lever, A.B.P. AND Pietro, W.J., "First-principle interpretation of ligand electrochemical (EL(L)) parameters. Factorization of the .sigma. and .pi. donor and .pi. acceptor capabilities of ligands," *J. Am. Chem. Soc.*1995; 117(26), 6990.

Anil Kumar Soni." sd-Hybridization, Population Analysis And MOT In Ru2+. I. Simple Ruthenium Dihalides." IOSR Journal of Engineering (IOSRJEN), vol. 09, no. 12, 2019, pp. 28-37.